AIP Journal of Applied Physics

Nanogrowth twins and abnormal magnetic behavior in CoFe 2 O 4 epitaxial thin films

Li Yan, Yu Wang, Jiefang Li, Alexander Pyatakov, and D. Viehland

Citation: Journal of Applied Physics **104**, 123910 (2008); doi: 10.1063/1.3033371
View online: http://dx.doi.org/10.1063/1.3033371
View Table of Contents: http://scitation.aip.org/content/aip/journal/jap/104/12?ver=pdfcov
Published by the AIP Publishing

Nanogrowth twins and abnormal magnetic behavior in $CoFe_2O_4$ epitaxial thin films

Li Yan,[1,a)] Yu Wang,[1] Jiefang Li,[1] Alexander Pyatakov,[2] and D. Viehland[1]
[1]*Department of Materials Science and Engineering, Virginia Tech, Blacksburg, Virginia 24061, USA*
[2]*Department of Physics, Moscow State University, Leninskie gori, 38, Moscow 119992, Russia*

(Received 1 July 2008; accepted 14 October 2008; published online 22 December 2008)

Nanogrowth twins (GTs) have been observed in $CoFe_2O_4$ (CFO) epitaxial thin films deposited on (111) oriented $SrTiO_3$ substrates by pulsed laser deposition. The GTs form during nucleation and growth and consist of CFO growth regions that have a mirror relationship with respect to each other. We show that the films with GTs (i) are better crystallized than the ones without them and (ii) have higher saturation magnetizations due to the presence of twin boundaries. © *2008 American Institute of Physics*. [DOI: 10.1063/1.3033371]

I. INTRODUCTION

Cobalt ferrite $CoFe_2O_4$ (CFO) is a magnetic oxide with the spinel structure, which has a cubic close packed (CCP) oxygen framework structure. Early studies of bulk CFO revealed that it tended to form a partially inverse spinel structure, where the degree of site inversion depended on thermal treatment:[1] $(Co_{0.07}Fe_{0.93})[Co_{0.93}Fe_{1.07}]O_4$ in a slow cooled condition and $(Co_{0.24}Fe_{0.76})[Co_{0.76}Fe_{1.24}]O_4$ in a quenched one (the parentheses indicate tetrahedral *A* sites and the square brackets indicate octahedral *B* sites). The spins of ions on *A* and *B* sites partially cancel each other. Spinel ferrites are unique among magnetic materials simultaneously having high resistivities, high Néel temperatures, high saturation magnetizations, and high permeabilities. Consequently, they are a material of choice for various magnetic applications ranging from high frequency devices to magneto-optical recording, and to microelectromechanical systems.[2–5]

There are two kinds of magnetic exchange interactions in spinel ferrites: (i) a direct *M-M* interaction J^d between two cations and (ii) a *M-O-M* superexchange interaction J^s_φ.[6] Experimentally, it has been found that the direct interaction J^d is favored when $\varphi \approx 90°$, whereas J^s_φ dominates from $90° \leq \varphi \leq 180°$. The anisotropy of the superexchange can be given as

$$J^s_\varphi = J^s_{90} \sin^2 \varphi + J^s_{180} \cos^2 \varphi. \quad (1)$$

When $\varphi \approx 180°$, an antiferromagnetic exchange that is proportional to $\cos^2 \varphi$ is favored; whereas when $\varphi \approx 90°$, a ferromagnetic exchange that is proportional to $\sin^2 \varphi$ is favored.[6–9] Several papers have previously been published on superexchange interactions in CFO.[10–14] The effect of heat treatment on superexchange interaction is known to be quite small, which means that the interaction is not so sensitive to whether Co occupies *A* or *B* sites.[10]

Various ferrite thin films (CFO, Fe_3O_4, $NiFe_2O_4$, $MnFe_2O_4$, etc.) have been grown on numerous substrates (MgO, $SrTiO_3$, $MgAl_2O_4$, etc.) by many deposition methods [sputtering, sol-gel, pulsed laser deposition (PLD), etc.].[2–5] Previously, studies of single crystal Fe_3O_4 films grown on MgO substrates by Margulies *et al.*[15,16] reported a local enhancement in the intrasublattice antiferromagnetic superexchange over that of the intersublattice in the vicinity of antiphase boundaries (APBs). Such APBs have been reported in Fe_3O_4 films grown on MgO by various deposition methods including solid state,[17] chemical vapor deposition,[18] PLD,[19] and molecular beam epitaxy.[20] These APBs are stacking faults *inherited* from film nucleation and growth. Such faults across APBs were shown to enhance the 180° *B-O-B* (intrasublattice) antiferromagnetic superexchange. Other types of stacking defects, such as twin boundaries, are known in ferromagnetic (magnetostrictive) and ferroelectric (piezoelectric) perovskite oxides.[21–26] In magnetostrictive oxides with high Néel temperatures (such as CFO), such twin boundaries could readily form in epitaxial thin layers during crystallization, annealing, or thermal treatments.

Growth twins (GTs) could offer another possible means to enhance the superexchange in CFO or other spinel ferrites. In this letter, we report the presence of GTs in ferromagnetic CFO thin films deposited on (111) oriented perovskite substrates. The GTs were identified by x-ray diffraction (XRD) and were shown to be of the order of tens of nanometers in size by electron microscopies. In addition, we show that films with such nano GTs have higher saturation magnetizations compared to those that are untwined.

II. EXPERIMENT

We deposited CFO layers by PLD on (001), (110), and (111) oriented $SrTiO_3$ (STO) with thickness of 140 nm. Heterostructures with $SrRuO_3$ (SRO) and/or $Pb(Zr,Ti)O_3$ (PZT) layers (50 nm thick) sandwiched between STO substrate and CFO films were also prepared, buffering the lattice mismatch between film and substrate. All films were deposited by a Lambda 305i KrF laser (wavelength of 248 nm), focused to a spot size of 2 mm^2, and incident on the surface of a target using energy densities of 1.2, 1.6, and 2.0 J/cm^2 for SRO, PZT, and CFO, respectively. The distance between the substrate and target was 6 cm, and the base vacuum of the chamber was $<10^{-5}$ Torr. During film deposition, the oxygen pressure was 150 mTorr for SRO, and 60 mTorr for PZT and

a)Electronic mail: lyan@vt.edu.

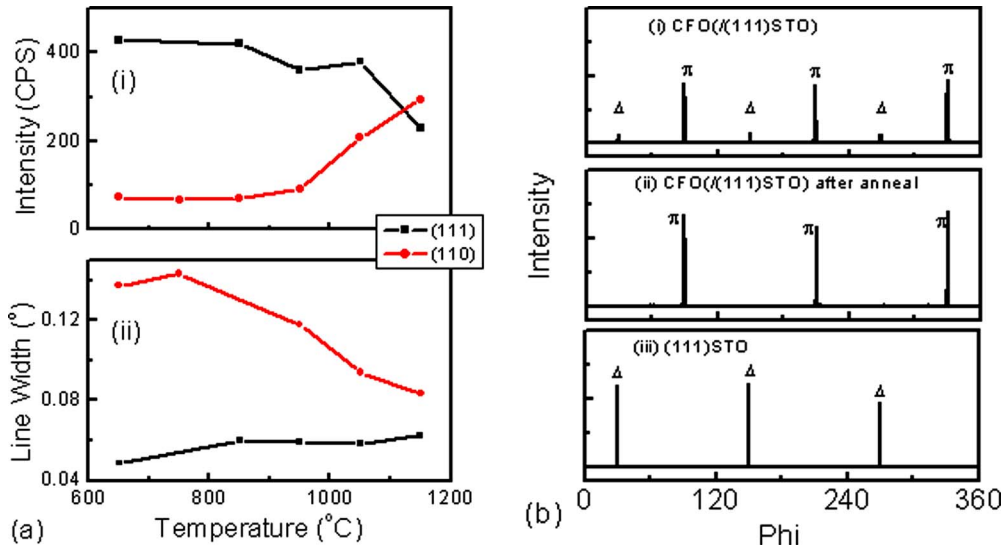

FIG. 1. (Color online) XRD, AFM, and SEM results of CFO thin film. (a) (i) Intensity and (ii) full width at half maximum of 2θ-ω line scan of (440) peak of (110) oriented CFO thin films (red dots) and (222) peak of (111) oriented CFO thin films (black dots) as a function of annealing temperature, demonstrating trend of crystallization. (b) Phi scan of (i) (440) peaks of as-grown (111) oriented CFO thin film, (ii) (440) peaks of after annealed (111) oriented CFO thin film, and (iii) (110) peaks of (111) oriented STO substrate.

CFO. The crystal structure of the films was measured using a Philips X'pert high resolution x-ray diffractometer equipped with a two bounce hybrid monochromator and an open three-circle Eulerian cradle. The analyzer was a Ge (220) cut crystal which had a θ-resolution of 0.0068°. The x-ray unit was operated at 45 kV and 40 mA with a wavelength of 1.5406 Å (Cu $K\alpha$). The magnetic properties of the CFO layers at 5 K were measured using a superconducting quantum interference device (SQUID) (Quantum Design MPMS magnetometer). The surface topology of CFO layers was studied by atomic force microscopy (AFM) (Veeco 3100) and scanning electron microscopy (SEM) (LEO 1550).

III. RESULTS AND DISCUSSION

First, we investigated the structure of (111) and (110) CFO films by XRD. Line scans revealed that all of our thin films were epitaxial single crystals (data not shown). Figure 1(a) summarizes the effect of annealing temperature: the integrated intensity of the corresponding principal reflection can be seen to be low in as-deposited (110) films (650 °C) but to increase with increasing annealing temperature, whereas it was initially high in the as-deposited (111) films and decreased slightly with increasing annealing temperature. In addition, this figure shows that the linewidth was narrow in as-deposited (111) films and broadened slightly with increasing annealing temperature, whereas that of (110) films was initially broad but narrowed with increasing annealing temperature, approaching the same value as that of (111) films annealed at higher temperatures. These data demonstrate that the (111) films are well crystallized as deposited and that annealing is slightly detrimental to the crystal integrity. Whereas (110) films are not as well crystallized in the as-deposited condition but become better crystallized upon annealing.

We also observed an anomalous magnetization for CFO films deposited on (111) oriented STO substrates. Figure 2(a) shows the M-H response of (111) CFO/STO. It is important to note that the saturation magnetization (M_s) before annealing is higher than M_s after annealing. However, magnetization behavior of (110) CFO/STO is quite normal, which is similar to literatures reported,[27] that M_s before annealing is lower than that of after annealing, as shown in Fig. 2(b). By comparing the magnetization and crystallization results, we can see that the better the crystallization, the higher the magnetization.

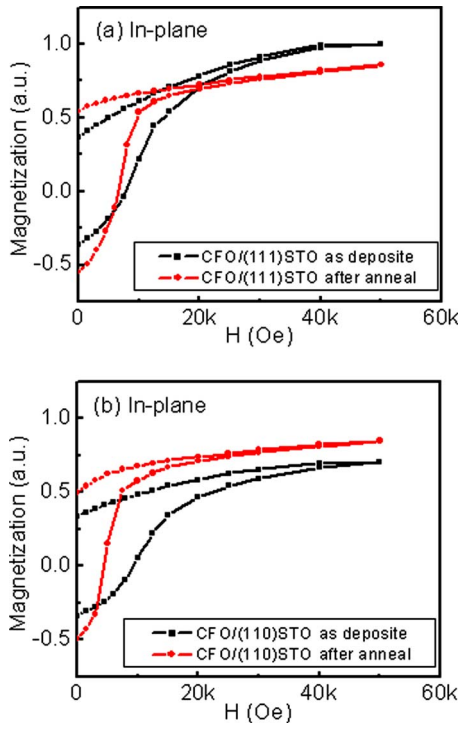

FIG. 2. (Color online) SQUID results of magnetization as a function of magnetic fields for (a) (111) and (b) (110) oriented CFO thin films as-grown (black dots) and after annealed (red dots) taken along the in-plane direction at 5 K.

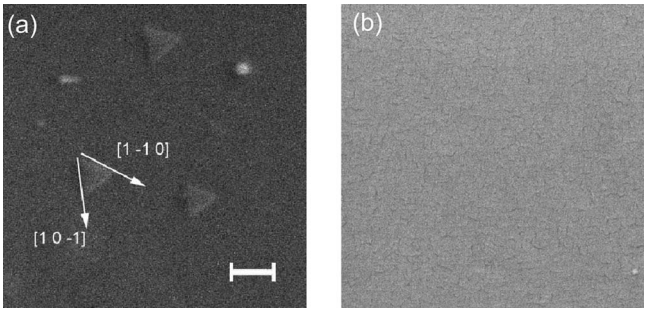

FIG. 3. (a) SEM image of as-grown (111) oriented CFO thin film demonstrating GTs, the bar is 100 nm, and (b) SEM image of after annealed (111) oriented CFO thin film.

It is natural to ask how annealing could make (111) CFO films apparently less crystallized, but (110) more. Figure 1(b) shows ϕ-scans taken from (i) (111) CFO/STO before annealing, (ii) (111) CFO/STO after annealing, and (iii) a STO substrate for comparison. The STO substrate reveals three equivalent peaks separated by 120°, marked by Δ in graph (iii) of this figure. This is consistent with a cubic lattice symmetry. We can also see that the annealed films had similar ϕ-scans, whose peaks were shifted by 60° with respect to the STO substrate lattice planes, as marked by π in graph (ii). Finally, we can see from graph (i) that the as-deposited films had three equivalent π peaks shifted by 60° and also a smaller fraction of three Δ peaks that were not shifted with respect to the substrate. The volume fraction of the Δ regions was $I_\Delta/(I_\Delta+I_\pi)\times 100\%=14\%$, where I is the relative diffraction intensity. We also obtained SEM images of (111) CFO films as given in Fig. 3(a) before annealing and in Fig. 3(b) after annealing. These images clearly reveal the presence of two growth regions in the as-deposited films, one with a triangular morphology of about 80 nm in size that is embedded within another. However, after annealing, only one region was observed. We also note that similar results were found for (111) CFO/PZT/STO and (111) CFO/SRO/STO, where the twin volume fraction was altered by the lattice mismatch with the buffer layer (data not shown). These results clearly show that the as-deposited (111) CFO films have two types of growth regions, which have the same out-of-plane [111] directions, but with their ⟨011⟩ and ⟨110⟩ axes rotated by 180° into mirror directions. Therefore, the minor Δ regions are epitaxial to the substrate, while the major π regions are twin-related to the substrate.

The formation of triangular Δ regions embedded in the π regions maybe a result of the anisotropic interfacial energy of the twin boundaries of the spinel crystal structure. After nucleation Δ and π regions seemingly grow on (111) substrates, impinging upon each other to form GT boundaries; triangular shapes with ⟨110⟩ edges may then form in order to minimize interfacial energy. We conceptually illustrate the twin boundary structure between the two types of growth regions for our as-deposited (111) CFO/STO, as given in Fig. 4(a), which shows a top view of the morphology consisting of triangular GTs embedded in a matrix, similar to the image in Fig. 3(a). These triangles represent the Δ epitaxial regions and the matrix, the π GT regions. Two types of atomic structures in the planes across the twin boundary between Δ and

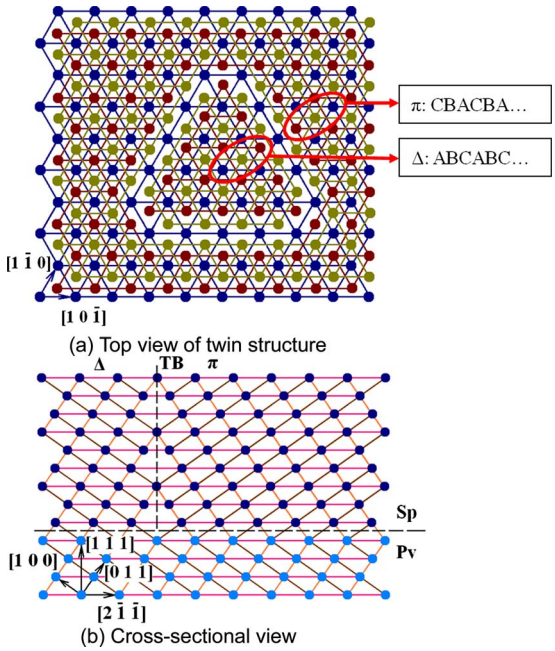

FIG. 4. (Color online) Stacking methods of oxygen ions across GTs in CFO thin films. (a) Top view of the GT structure and (b) cross-sectional view of GT, which is grown in $(01\bar{1})$ plane, where the bottom is the perovskite substrate, the top is the spinel thin film, the top left is Δ regions, and the top right is π regions demonstrating the possible stacking methods of oxygen ions in GTs.

π regions can be seen in Fig. 4(a), which have different oxygen stacking sequences: *ABCABC…ABC* and *CBACBA…CBA*.

The cross sections of one possible stacking sequences of GTs in (111) CFO films are schematically illustrated in Fig. 4(b), which correspond to twin boundaries in $(01\bar{1})$ planes. The $(01\bar{1})$ twin boundaries are created normal to the substrate. It should also be noted that there is a difference between GT boundaries and APBs; across an APB the oxygen framework is not disturbed rather only *A* and/or *B* site cations are slipped. Accordingly, one cannot observe APBs by XRD but rather only by electron microscopy. Whereas, GTs twist their oxygen frameworks, which can be detected by XRD by a peak shift. Figure 2 also illustrates that the π regions have a stacking sequence that is rotated by 180° with respect to the STO substrate, producing a mirror growth plane (twin plane) at the film/substrate interface, whereas the Δ regions have a stacking sequence, which continues that of the substrate on which it grows. The Δ regions nucleate epitaxial to the substrate, whereas the π regions nucleate on a mirror plane to it. Across the boundaries, the oxygen stacking sequences are mirror related to each other. Furthermore, results also show that annealing (111) CFO films drives out GT boundaries. Dislocations and point defects are confined in the twin boundary regions during film deposition; thus the films are better crystallized before annealing. During annealing at 1050 °C, diffusion may result in the movement of twin boundaries and shrinkage of the minor regions, reducing interfacial energies; only the mirror growth regions of CFO films on STO substrates persist.

The preference for mirror growth regions can be attributed to the stacking sequence difference between spinel and perovskite structures at their interface. The oxygen stacking sequence of spinel is *ABCABC…ABC*, whereas perovskite has the same sequence but requires that $\frac{1}{3}$ of the oxygen ions are missing, substituted by M^{4+} on the *B* sites. The reason why such twin boundaries are only found in (111) oriented CFO thin films is that (111) is the CCP plane; thus twinned boundaries are generated when the first two layers are mismatched, which does not happen for (001) and (110) oriented CFO films grown on STO substrate.

IV. CONCLUSIONS

In summary, we have found that as-grown (111) CFO films deposited on STO are (i) better crystallized and (ii) have higher magnetization than after annealing. The reason is the nanogrowth twin structure in (111) CFO/STO thin films.

ACKNOWLEDGMENTS

We would like to gratefully acknowledge financial support from the U.S. Department of Energy under Contract No. DE.-AC02-98CH10886, Office of the Air-Force, Office of Scientific Research under Grant No. FA 9550-06-1-0410, the Office of Naval Research under Grant No. N00014-06-1-0204 and RFBR 05-02-16997-a, and the Dynasty Foundation.

[1]G. A. Sawatzky, F. V. D. Woude, and A. H. Morrish, Phys. Rev. **187**, 747 (1969).
[2]Y. C. Wang, J. Ding, J. B. Yi, B. H. Liu, T. Yu, and Z. X. Shen, Appl. Phys. Lett. **84**, 2596 (2004).
[3]P. C. Dorsey, P. Lubitz, D. B. Chrisey, and J. S. Horwitz, J. Appl. Phys. **79**, 6338 (1996).
[4]Y. Suzuki, R. B. van Dover, E. M. Gyorgy, J. M. Phillips, V. Korenivski, D. J. Werder, C. H. Chen, R. J. Cava, J. J. Krajewski, W. F. Peck, Jr., and K. B. Bo, Appl. Phys. Lett. **68**, 714 (1996).
[5]Y. Suzuki, R. B. van Dover, E. M. Gyorgy, J. M. Phillips, V. Korenivski, D. J. Werder, C. H. Chen, R. J. Felder, R. J. Cava, J. J. Krajewski, and W. F. Peck, Jr., J. Appl. Phys. **79**, 5923 (1996).
[6]K. Motida and S. Miyahara, J. Phys. Soc. Jpn. **28**, 1188 (1970).
[7]G. A. Sawatzky, W. Geertsma, and C. Haas, J. Magn. Magn. Mater. **3**, 37 (1976).
[8]J. Kanamori, J. Phys. Chem. Solids **10**, 87 (1959).
[9]J. B. Goodenough, Phys. Rev. **100**, 564 (1955).
[10]S. J. Kim, S. W. Lee, S. Y. An, and C. S. Kim, J. Magn. Magn. Mater. **215–216**, 210 (2000).
[11]R. M. Persoons, E. D. Grave, P. M. A. de Bakker, and R. E. Vandenberghe, Phys. Rev. B **47**, 5894 (1993).
[12]E. De Grave, R. M. Persoons, R. E. Vandenberghe, and P. M. A. de Bakker, Phys. Rev. B **47**, 5881 (1993).
[13]C. M. Srivastava, G. Srinivasan, and N. G. Nanadikar, Phys. Rev. B **19**, 499 (1979).
[14]C. Zener, Phys. Rev. **82**, 403 (1951).
[15]D. T. Margulies, F. T. Parker, M. L. Rudee, F. E. Spada, J. N. Chapman, P. R. Aitchison, and A. E. Berkowitz, Phys. Rev. Lett. **79**, 5162 (1997).
[16]D. T. Margulies, F. T. Parker, F. E. Spada, R. S. Goldman, J. Li, R. Sinclair, and A. E. Berkowitz, Phys. Rev. B **53**, 9175 (1996).
[17]D. Hesse, J. Vac. Sci. Technol. A **5**, 1696 (1987).
[18]A. G. Fitzgerald and T. G. May, Thin Solid Films **35**, 201 (1976).
[19]S. Ramamurthy, P. G. Kotula, and C. B. Carter, *Polycrystalline Thin Films: Structure, Texture, Properties and Applications*, MRS Symposia Proceedings No. 343 (Materials Research Society, Pittsburgh, 1994), p. 517.
[20]J. M. Gaines, J. T. Kohlhepp, P. J. H. Bloemen, R. M. Wolf, A. Reinders, and R. M. Jungblut, J. Magn. Magn. Mater. **165**, 439 (1997).
[21]D. Shilo, G. Ravichandran, and K. Bhattacharya, Nature (London) **3**, 453 (2004).
[22]M. W. Chu, I. Szafraniak, D. Hesse, M. Alexe, and U. Gösele, Phys. Rev. B **72**, 174112 (2005).
[23]A. Khapikov, L. Uspenskaya, I. Bdikin, Ya. Mukovskii, S. Karabashev, D. Shulyaev, and A. Arsenov, Appl. Phys. Lett. **77**, 2376 (2000).
[24]G. Jung, V. Markovich, D. Mogilyanski, C. van der Beek, and Y. M. Mukovskii, J. Magn. Magn. Mater. **290–291**, 902 (2005).
[25]Y. U. Wang, Phys. Rev. B **74**, 104109 (2006).
[26]Y. U. Wang, Phys. Rev. B **73**, 014113 (2006).
[27]Y. Suzuki, Annu. Rev. Mater. Res. **31**, 265 (2001).